

Renormalization-group approach to nonequilibrium Green functions in correlated impurity systems

T. A. Costi*

Institut Laue-Langevin, Boîte Postale 156, 38042 Grenoble, Cedex 9, France

and Universität Karlsruhe, Institut für Theorie der Kondensierten Materie, 76128 Karlsruhe, Germany†

(Received 22 August 1996; revised manuscript received 1 October 1996)

We present a technique for calculating nonequilibrium Green functions for impurity systems with local interactions. We use an analogy to the calculation of response functions in the x-ray problem. The initial-state and the final-state problems, which correspond to the situations before and after the disturbance (an electric or magnetic field, for example) is suddenly switched on, are solved with the aid of Wilson's momentum shell renormalization group. The method is illustrated by calculating the nonequilibrium dynamics of the Ohmic two-state problem. [S0163-1829(97)00205-1]

I. INTRODUCTION

Recently there has been interest in the nonequilibrium transport properties of small devices, such as quantum dots and ultrasmall tunnel junctions.^{1,2} These systems, together with some resonant tunneling devices,³ offer possibilities for studying many-body effects due to strong local Coulomb interactions. The importance of these interactions in small devices is seen, for example, in the suppression of tunneling or the Coulomb blockade effect.⁴ Phenomena such as the Kondo effect in quantum dots and the Fermi edge singularity in resonant tunneling devices have been predicted⁵⁻¹¹ and some aspects of these have been confirmed experimentally.³ The usual starting point for dealing with nonequilibrium transport in such systems has been the formalism developed by Keldysh¹² and Kadanoff and Baym.¹³ Below we describe a nonperturbative approach based on the numerical renormalization-group (NRG) method,^{14,15} which allows the calculation of nonequilibrium Green functions for the above systems. We consider only the case in which the perturbation (an electric or magnetic field) causing the nonequilibrium effects is suddenly switched on at time $t=0$. The nonequilibrium Green functions will then be calculated by solving an initial- ($t<0$) and final- ($t>0$) state problem as in the case of calculating the photoemission and absorption spectra in the x-ray problem.¹⁶ In this paper we concentrate on calculating the nonequilibrium properties of a specific model, the Ohmic two-state system.¹⁷ The application of the method to the systems mentioned above follows along the same lines, the only difference being the solution, using the NRG method, of different initial- and final-state Hamiltonians.

The paper is organized as follows: in Sec. II we introduce the standard model of the Ohmic two-state system, formulate the problem of calculating the nonequilibrium dynamics of this model in terms of solving an initial- and a final-state problem and introduce an equivalent model, the anisotropic Kondo model, which we actually use in the calculations. In Sec. III we describe the NRG, its application to dynamical quantities and an approximate evaluation of the formally exact expressions for the nonequilibrium quantities. An exact evaluation of nonequilibrium quantities first has to overcome certain technical difficulties, which we describe, and is postponed for the future. Section IV contains our results for the

nonequilibrium dynamics of the Ohmic two-state system, obtained on the basis of NRG calculations for the anisotropic Kondo model. In Sec. V we summarize our main conclusions.

II. FORMULATION

A. The Ohmic two-state system

The nonequilibrium properties of the Ohmic two-state problem are of main interest in macroscopic quantum coherence experiments in rf superconducting quantum interference devices (SQUID's).¹⁸ Typically, an rf SQUID can be in one of two possible fluxoid states. By applying a bias (corresponding to an external magnetic field), for times $t<0$, the system is prepared in one of the two states. The dynamics after the bias is removed at $t>0$ is then intrinsically a nonequilibrium property. The Hamiltonian, H , of the system is time dependent with a sudden perturbation at $t=0$, so that we can write $H(t)=[1-\theta(t)]H_I+\theta(t)H_F$ where H_I, H_F are the Hamiltonians before and after the bias is switched off. The Hamiltonian $H_{I,F}$ describing the Ohmic two-state system is given by the spin-boson model,¹⁹

$$H_{\text{SB}} = -\frac{1}{2}\hbar\Delta\sigma_x + \frac{1}{2}\epsilon\sigma_z + \sum_{\alpha}\omega_{\alpha}\left(a_{\alpha}^{\dagger}a_{\alpha} + \frac{1}{2}\right) + \frac{1}{2}q_0\sigma_z\sum_{\alpha}\frac{C_{\alpha}}{\sqrt{2m_{\alpha}\omega_{\alpha}}}(a_{\alpha}+a_{\alpha}^{\dagger}). \quad (1)$$

Here $\sigma_i, i=x,y,z$ are Pauli spin matrices, the two states of the system correspond to $\sigma_z=\uparrow$ and $\sigma_z=\downarrow$ (i.e., $\sigma_z=\uparrow, \downarrow$ correspond to the two possible fluxoid states of the rf SQUID). Δ is the bare tunneling matrix element and ϵ is a bias. The environment is represented by an infinite set of harmonic oscillators (labeled by the index α) with masses m_{α} and frequency spectrum ω_{α} coupling linearly to the coordinate $Q=(1/2)q_0\sigma_z$ of the two-level system via a term characterized by the couplings C_{α} (the two-level system coordinate could be the total flux, $\phi=\phi_1\sigma_z$, in the case of an rf SQUID experiment). The environment spectral function is given in terms of these couplings, oscillator masses and frequencies by $J(\omega)=(\pi/2)\sum_{\alpha}(C_{\alpha}^2/m_{\alpha}\omega_{\alpha})\delta(\omega-\omega_{\alpha})$. In the

case of an Ohmic heat bath, of interest to us here, we have $J(\omega) = 2\pi\alpha\omega$, for $\omega \ll \omega_c$, where ω_c is a high-energy cutoff and α is a dimensionless parameter characterizing the strength of the dissipation. This form for the spectral function is appropriate for describing quantum dissipation in an rf SQUID. Preparation of the system in a state with $\sigma_z = +1$ with the oscillators relaxed about this state is equivalent to setting $\epsilon = -\infty$ in H_{SB} , so the initial-state problem corresponds to solving $H_I = H_{SB}(\epsilon = -\infty)$. Similarly, the final-state problem is given by $H_F = H_{SB}(\epsilon = 0)$. The Ohmic spin-boson model has been intensively studied (for reviews we refer the reader to Refs. 19,20). We outline some of its features in order to introduce some useful notation. The model has a low-energy scale, $\Delta_r < \Delta$ for $\Delta \ll \omega_c$, which depends on the dissipation strength α , and which may be interpreted as a renormalized tunneling amplitude. For $\alpha \ll 1$ the dynamics corresponds to damped oscillations, with a crossover to incoherent behavior with increasing dissipation strength. For $\alpha \rightarrow 1^-$, the renormalized tunneling amplitude vanishes giving rise to the phenomenon of ‘‘localization’’ or ‘‘self-trapping’’ for $\alpha > \alpha_c \approx 1$ (α_c depends also on the precise value of Δ). The dynamical quantities exhibiting the above features are defined below.

B. Nonequilibrium dynamical quantities

The simplest nonequilibrium dynamical quantity to study for the spin-boson model is the quantity $P(t) = \langle \sigma_z(t) \rangle_{\rho_I}$,¹⁹ where the thermodynamic average is taken with respect to the initial density matrix $\rho_I(\beta) = e^{-\beta H_I} / \text{Tr} e^{-\beta H_I}$, β is the inverse temperature, and the time evolution is with respect to the Hamiltonian after the bias is switched off at time $t = 0$, i.e., $\sigma_z(t) = e^{iH_F t} \sigma_z e^{-iH_F t}$. Hence, $P(t) = 1$ for $t < 0$ due to the infinite bias $\epsilon = -\infty$, and for $t > 0$, when the bias is switched off ($\epsilon = 0$), $P(t)$ describes how the two-level system coordinate σ_z relaxes to its long-time value of zero. Another quantity of interest is the retarded two-time Green function, $G_r(t, t') = -i\theta(t - t') \langle [\sigma_z(t), \sigma_z(t')] \rangle_{\rho_I}$, with the thermodynamic average defined as above. Since time translational invariance is broken, $G_r(t, t')$ depends on both times explicitly. We consider the Fourier transform of $G_r(t, t')$ with respect to both the sum $t + t'$ and difference $t - t'$ of the time variables. The resulting spectral density $C_r(\omega, \Omega) = -(1/\pi) \text{Im} G_r(\omega + i\delta, \Omega)$, with ω, Ω the Fourier frequency variables corresponding to $t - t', t + t'$, is given within a Lehmann representation by the following expression:

$$C_r(\omega, \Omega) = \frac{2\pi}{Z_I} \sum_{m_I, m_F, m'_F, m''_F} e^{-\beta E_{m_I}} \langle m_I | m_F \rangle \langle m''_F | m_I \rangle \times \langle m_F | \sigma_z | m'_F \rangle \langle m'_F | \sigma_z | m''_F \rangle \delta \left(\Omega - \frac{E_{m_F} - E_{m''_F}}{2} \right) \times \left\{ \delta \left(\omega + \left[\frac{E_{m_F} + E_{m''_F}}{2} - E_{m'_F} \right] \right) - \delta \left(\omega - \left[\frac{E_{m_F} + E_{m''_F}}{2} - E_{m'_F} \right] \right) \right\}. \quad (2)$$

Here, E_{m_I} and $|m_I\rangle$ are the many-body eigenvalues and eigenstates of the initial-state Hamiltonian H_I , Z_I is the corresponding partition function, and E_{m_F} , $|m_F\rangle$, $E_{m'_F}$, $|m'_F\rangle, \dots$ are the many-body eigenvalues and eigenstates of the final-state Hamiltonian H_F . In the equilibrium case, $H_I = H_F = H$, and the corresponding spectral density $C_r^{\text{eq}}(\omega, \Omega)$ reduces to

$$C_r^{\text{eq}}(\omega, \Omega) = \frac{2\pi}{Z} \sum_{m, m'} e^{-\beta E_m} |\langle m | \sigma_z | m' \rangle|^2 \delta(\Omega) \times \{ \delta(\omega + [E_m - E_{m'}]) - \delta(\omega - [E_m - E_{m'}]) \}, \quad (3)$$

where $E_m, |m\rangle$ are the many-body eigenvalues and eigenfunctions of H and Z is the corresponding partition function [the delta function, $\delta(\Omega)$, in the above expression reflects the fact that in the equilibrium case, $G_r(t, t')$ depends only on the difference of the time variables].

We see that the nonequilibrium spectral density differs from the equilibrium one in several ways: first, even at $T = 0$, no ground-state energy appears in the δ functions, the excitations are between arbitrary (final) excited states of the system. This reflects the fact that there is no stationary ground-state for a nonequilibrium situation. Secondly, the nonequilibrium aspects, which are a result of an initial-state preparation, are reflected in the presence of overlap matrix elements between the initial and final states. Finally the dependence on Ω is a measure of the importance of transient effects. Neglecting these effects results in the following simplified expression for the spectral density:

$$C_{0,r}(\omega) = C_r(\omega, \Omega = 0) = \frac{2\pi}{Z_I} \sum_{m_I, m_F, m'_F} e^{-\beta E_{m_I}} |\langle m_I | m_F \rangle|^2 |\langle m_F | \sigma_z | m'_F \rangle|^2 \times \delta(\Omega) \{ \delta(\omega + [E_{m_F} - E_{m'_F}]) - \delta(\omega - [E_{m_F} - E_{m'_F}]) \}. \quad (4)$$

This describes the steady-state case $t + t' \rightarrow \infty$. In a strict sense it is not a nonequilibrium quantity, although it does take into account the effects of an initial-state preparation on the correlation function $\langle \sigma_z(t) \sigma_z(0) \rangle$. Our motivation for calculating this quantity is simply to illustrate that our technique applies also to two-time Green functions. The calculation of the full spectral density $C_r(\omega, \Omega)$, including both frequencies involves a straightforward generalization.

Similarly we can write the Fourier transform of $P(t)$, within a Lehmann representation, as

$$P(\omega) = \frac{1}{Z_I} \sum_{m_I, m_F, m'_F} e^{-\beta E_{m_I}} \langle m_I | m_F \rangle \langle m'_F | m_I \rangle \times \langle m_F | \sigma_z | m'_F \rangle \delta(\omega - (E_{m_F} - E_{m'_F})), \quad (5)$$

where the same notation as above is used.

$P(t) = \int_0^\infty P(\omega) \cos(\omega t) dt$ contains information on the onset of quantum oscillations in the two-level system. For small values of the dissipation strength, $\alpha \ll 1$, it is known

from the noninteracting blip approximation¹⁹ (NIBA) that $P(t)$ exhibits damped oscillations with a renormalized tunneling frequency $\Delta_r = \Delta[\Delta/\omega_c]^{\alpha/(1-\alpha)}$. $P(\omega)$ will exhibit two peaks at $\omega = \pm \Delta_r$. At the exactly solvable Toulouse point,²¹ $\alpha = 1/2$, where the Ohmic two-state system reduces to the resonant-level model,^{19,22} the dynamics is incoherent and $P(t)$ decays exponentially. $P(\omega)$ consists of a single peak at $\omega = 0$. It is not clear at which value of the dissipation strength the crossover to incoherent behavior occurs, in particular whether it occurs at exactly $\alpha = 1/2$ or for some smaller value of α . This may depend on the definition of the crossover and on whether equilibrium or nonequilibrium quantities are being studied. For equilibrium quantities a smooth crossover has been found to occur at $\alpha = 1/3$.^{24,28}

C. The anisotropic Kondo model

Instead of solving directly the spin-boson model with the NRG method it is more convenient to solve an equivalent fermionic model which has the same dynamics. This is the anisotropic Kondo model (AKM). The equivalence has been shown at the Hamiltonian level via bosonization.²³ This was believed to be valid in the region $\alpha > 1/2$, which corresponds (see below for the precise statement of the equivalence) to the region in the parameter space of the AKM between weak coupling and the Toulouse point. In fact, recent work²⁴ shows that the equivalence extends beyond the Toulouse point into the region describing weak dissipation $0 < \alpha < 1/2$ (or large antiferromagnetic J_{\parallel} in the AKM, see also Ref. 25). The AKM is given by²⁶

$$H = \sum_{k,\sigma} \epsilon_k c_{k\sigma}^\dagger c_{k\sigma} + \frac{J_{\perp}}{2} \sum_{kk'} (c_{k\uparrow}^\dagger c_{k'\downarrow} S^- + c_{k\downarrow}^\dagger c_{k'\uparrow} S^+) + \frac{J_{\parallel}}{2} \sum_{kk'} (c_{k\uparrow}^\dagger c_{k'\uparrow} - c_{k\downarrow}^\dagger c_{k'\downarrow}) S^z + g \mu_B h S_z. \quad (6)$$

The first term represents noninteracting conduction electrons and the second and third terms represent an exchange interaction between a localized spin 1/2 and the conduction electrons with strength J_{\perp}, J_{\parallel} . A local magnetic field h , coupling only to the impurity spin in the Kondo model [the last term in Eq. (6)], corresponds to a finite bias ϵ in the spin-boson model. The correspondence between H and H_{SB} is then given by $\epsilon = g \mu_B h$, $\Delta/\omega_c = \rho J_{\perp}$ and $\alpha = (1 + 2\delta/\pi)^2$, where $\tan \delta = -\pi \rho J_{\parallel}/4$, δ is the phase shift for scattering of electrons from a potential $J_{\parallel}/4$ and $\rho = 1/2D$ is the conduction-electron density of states per spin at the Fermi level for a flat band of width $2D$.^{19,24} We note that weak dissipation ($\alpha \rightarrow 0$) in the spin-boson model corresponds to extreme anisotropy ($J_{\parallel} \rightarrow \infty$) in the Kondo model. For zero dissipation, $J_{\parallel} = \infty$, the two states $\psi_{\pm} = 1/\sqrt{2}(|\uparrow\rangle|\downarrow\rangle_0 \pm |\downarrow\rangle|\uparrow\rangle_0)$ made up from the impurity states and the local conduction-electron Wannier orbitals $|\sigma\rangle_0 = \sum_k c_{k\sigma}^\dagger |\text{vac}\rangle$, where $|\text{vac}\rangle$ is the vacuum, are split by $J_{\perp} = \Delta$ (with the identification $\omega_c = 2D$) and are completely decoupled from the rest of the conduction band, thus forming an isolated two-level system. The system exhibits coherent oscillations with $P(t) = \cos(\Delta t)$. As J_{\parallel} is decreased from $+\infty$, the two levels become weakly coupled, with strength $D^2/J_{\parallel} \propto \alpha$, for $\rho J_{\parallel} \gg 1$, to the remaining conduction states and their splitting is

renormalized downwards. The low-energy scale of the model is given by the Kondo temperature for the anisotropic Kondo model,²⁷ $T_K(J_{\perp}, J_{\parallel}) < J_{\perp}$, for $J_{\perp} \ll D$, which in the language of the dissipative two-state system corresponds to a renormalized tunneling amplitude Δ_r .²⁴ An extensive discussion of the equivalence between the anisotropic Kondo model and the Ohmic two-state system is given elsewhere.

III. CALCULATION OF NONEQUILIBRIUM DYNAMICS VIA THE NRG

A. The NRG

The dynamical quantities $P(t)$ and $G_r(t, t')$ defined above for the two-level system translate into the corresponding quantities for the Kondo model ($\sigma_z \rightarrow S_z$ under the equivalence). We calculate these quantities by applying Wilson's momentum shell renormalization-group method generalized to the calculation of dynamical quantities (e.g., Refs. 24,29). Thus in addition to solving an initial-state problem $H_I = H_{\text{AKM}}(\epsilon = -\infty)$ and a final-state problem $H_F = H_{\text{AKM}}(\epsilon = 0)$, the final-state matrix elements of the variable σ_z and the overlap matrix elements appearing in the above expressions for $P(\omega), C_r(\omega)$ are also calculated. The diagonalization of H_{AKM} proceeds as follows (for full details see Ref. 14): (i) the spectrum is linearized about the Fermi energy $\epsilon_k \rightarrow v_F k$, (ii) a logarithmic mesh of k points $k_n = \Lambda^{-n}$ is introduced to achieve a separation of energy scales, and (iii) a unitary transformation of the $c_{k\sigma}$ is made such that $f_{0\sigma} = \sum_k c_{k\sigma}$ is the first operator in a new basis, $f_{n\sigma}, n = 0, 1, \dots$, which tridiagonalizes $H_c = \sum_{k\mu} \epsilon_{k\mu} c_{k\mu}^\dagger c_{k\mu}$ in k space, i.e., $H_c \rightarrow \sum_{\mu} \sum_{n=0}^{\infty} \xi_n \Lambda^{-n/2} (f_{n+1\mu}^\dagger f_{n\mu} + \text{H.c.})$, with $\xi_n \rightarrow (1 + \Lambda^{-1})/2$ for $n \gg 1$. The Hamiltonian (6) with the above discretized form of the kinetic energy is now diagonalized by the following iterative process: (a) one defines a sequence of finite-size Hamiltonians $H_N = \sum_{\mu} \sum_{n=0}^{N-1} \xi_n \Lambda^{-n/2} (f_{n+1\mu}^\dagger f_{n\mu} + \text{H.c.}) + J_{\perp}/2 (f_{0\uparrow}^\dagger f_{0\downarrow} S^- + f_{0\downarrow}^\dagger f_{0\uparrow} S^+) + J_{\parallel}/2 (f_{0\uparrow}^\dagger f_{0\uparrow} - f_{0\downarrow}^\dagger f_{0\downarrow}) S^z$ for $N \geq 0$; (b) the Hamiltonians H_N are rescaled by $\Lambda^{(N-1)/2}$ such that the energy spacing remains the same, i.e. $\bar{H}_N = \Lambda^{(N-1)/2} H_N$. This defines a renormalization-group transformation $\bar{H}_{N+1} = \Lambda^{1/2} \bar{H}_N + \sum_{\mu} \xi_N (f_{N+1\mu}^\dagger f_{N\mu} + \text{H.c.}) - E_{G,N+1}$, with $E_{G,N+1}$ chosen so that the ground-state energy of \bar{H}_{N+1} is zero. Using this recurrence relation, the sequence of Hamiltonians \bar{H}_N for $N = 0, 1, \dots$ is iteratively diagonalized. This gives the excitations and many-body eigenstates at a corresponding set of energy scales ω_N defined by $\omega_N = \Lambda^{-(N-1)/2}$ and allows a direct calculation of the dynamical quantities $P(t), G_r(t, t')$, or more precisely their Fourier transforms using the Lehmann representations (2,5). Our results were obtained for $\Lambda = 2$, keeping the 320 lowest states at each iteration. Truncating the spectrum in this way restricts the range of excitations ω at iteration N to be such that $\omega_N \leq \omega \leq K \omega_N$, where $K = K(\Lambda) \approx 7$ for $\Lambda = 2$. In this paper we discuss only the $T = 0$ results.

In diagonalizing the Hamiltonians \bar{H}_N the following symmetries are used to reduce the size of the matrices: (i) conservation of the z component of total spin $S_z^{\text{tot}} = S_z + \sum_{n=0}^N (1/2)(f_{n\uparrow}^\dagger f_{n\uparrow} - f_{n\downarrow}^\dagger f_{n\downarrow})$, (ii) conservation of total pseudospin,³⁰ where the pseudospin operators j^+, j^-, j_z

are defined by $j^+ = \sum_{n=0}^N (-1)^n f_{n\uparrow}^\dagger f_{n\downarrow}^\dagger$, $j^- = (j^+)^\dagger$ and $j_z = \sum_{n=0}^N (f_{n\mu}^\dagger f_{n\mu} - 1/2)$. These symmetries hold for both the zero and finite bias cases, which we consider in this paper ($\epsilon=0$ for the final-state problem and $\epsilon=-\infty$ for the initial-state problem). At this point we mention that although it is, in principal, possible to apply this renormalization-group method directly to the spin-boson model, in practice there are disadvantages in the case of the bosonic problem.³¹

B. Broadening procedure for the discrete spectra

We note that the use of a discretized model implies that at each iteration $P(\omega)$ is a series of δ functions. Smooth curves are obtained by broadening these δ functions with a Gaussian of width appropriate to the level spacing of H_N .²⁹ The width of the Gaussians will not influence the intrinsic peak widths at low energies, where the logarithmic spacing ensures high resolution, but may do so at higher energies where the resolution is lower. This problem has been discussed in detail in Ref. 33, where a refined NRG scheme to overcome it has been suggested. In most problems one is interested in the low-energy behavior and such a refinement is not required, however for the spin-boson model considered here there is interesting dynamics at high energies and such a refinement is required in order to obtain a complete description of all aspects of the high energy (short time) dynamics (by high energy, we mean high relative to the renormalized tunneling amplitude, but still low relative to the high-energy cutoff in the model). In the present paper we have not implemented the above refined scheme, so we shall state below which aspects of the high-energy dynamics we are able to obtain within the unmodified NRG scheme.

C. Approximate evaluation of nonequilibrium quantities

At this stage we point out an important difference in the calculation of nonequilibrium quantities with respect to equilibrium quantities such as $C_r^{\text{eq}}(\omega, \Omega)$. At $T=0$, the latter can be calculated on each energy scale ω_N by restricting attention to a single energy shell N . This is due to the existence of a stationary ground state, from which all excitations in the expression for C_r^{eq} can be measured. The δ functions in the Lehmann representation, Eq. (3), then imply that in order to calculate C_r^{eq} at frequency ω , only one energy shell, that for which $\omega \approx \omega_N$, is required, i.e.,

$$C_r^{\text{eq}}(\omega, \Omega, T=0) = \frac{2\pi}{Z_N} \sum_{m'} |\langle \text{GS} | \sigma_z | m' \rangle_N|^2 \delta(\Omega) \times \{ \delta(\omega + [E_{\text{GS}}^N - E_{m'}^N]) - \delta(\omega - [E_{\text{GS}}^N - E_{m'}^N]) \}, \quad (7)$$

where $|m'\rangle_N$, $|\text{GS}\rangle_N$ are the eigenstates and the ground state, corresponding to iteration N in the NRG procedure, $E_{m'}^N$ and E_{GS}^N the corresponding eigenvalues, and Z_N the ($T=0$) partition function. Contributions from energy shells $n=0, 1, \dots, N-1$ have $E_m^n - E_{\text{GS}}^n > \omega$ so they make no contribution to the spectral density C_r^{eq} at frequency $\omega \approx \omega_N$. At

finite temperatures, there can be contributions from higher energy states, although the Boltzmann factors in Eq. (3) will suppress these.

The situation is different for nonequilibrium dynamical quantities, such as $P(\omega)$. From the Lehmann representation (5) we see that, even at $T=0$, no ground-state energy appears in the δ functions. Instead the ($T=0$) excitations are between arbitrary (final) states. The response at frequency $\omega \approx \omega_N$ can have contributions from all energy shells $n=0, 1, \dots, N$. Hence, if we evaluate $P(\omega)$, at the frequency $\omega \sim \omega_N = D\Lambda^{-(N-1)/2}$, by taking into account only the N th energy shell, we have only the *approximate* result

$$P(\omega) \approx P_N(\omega) = \frac{1}{Z_{N, I_{m_F}, m'_F}} \sum \langle m_{I, \text{GS}} | m_F \rangle_N \langle m'_F | m_{I, \text{GS}} \rangle_N \times \langle m_F | \sigma_z | m'_F \rangle_N \delta(\omega - (E_{m_F}^N - E_{m'_F}^N)). \quad (8)$$

The approximation implicit in this procedure is that small excitations $\omega \sim E_{m_F}^n - E_{m'_F}^n$ between higher energy excited states (i.e., from energy shells with $n < N$), make a negligible contribution to $P(\omega)$ compared to those on a scale $\omega \sim \omega_N$ from the N th energy shell. This is clearly only an approximation to the formally exact expression (5). The results and arguments to be presented below show that the above approximation has a regime of validity and a regime where it breaks down. We stress, however, that a full multiple-shell evaluation of Eq. (5) will ultimately be required. This is currently not feasible within the standard NRG procedure described in Secs. III A and III B. One first has to overcome two problems: (i) a possible double counting of excitations in adding contributions to $P(\omega)$ from different energy shells, (ii) a meaningful way of adding contributions to $P(\omega)$ from higher energy shells which have different resolutions. The second problem can be overcome by replacing the standard NRG procedure of Secs. III A and III B by one which eliminates any dependence of static and dynamic quantities on the logarithmic discretization.³³ These problems do not arise in the case of equilibrium dynamical quantities since, as discussed above, the spectral densities can be calculated essentially without approximation by restricting attention to just one energy shell for each frequency of interest²⁹ (although, as discussed in Sec. III B, the use of a logarithmic discretization and a Gaussian broadening procedure can overestimate the widths of high-energy peaks in spectral densities).

Returning to Eq. (8) we expect this to be a valid approximation as long as orthogonality effects do not significantly affect the overlap matrix elements $\langle m'_F | m_{I, \text{GS}} \rangle_N$ appearing in the above expression [and similar expressions for $C_{0r}(\omega)$]. When this occurs, as it will do for sufficiently low energies,³² an increasing number of final states $|m_F\rangle_N$ will be nearly orthogonal to the initial ground state $|m_{I, \text{GS}}\rangle_N$ and it will be necessary to include higher-energy states. Information on higher-energy states is contained in previous iterations within the NRG procedure. Thus if we evaluate the nonequilibrium quantities approximately by using only one energy shell, then we will obtain results with a restricted range of validity. The range of validity can be estimated: orthogonality effects between initial and final states become important in the strong-coupling regime, i.e., for frequencies $\omega \ll T_K$,

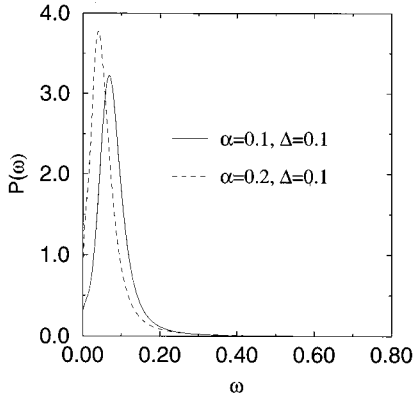


FIG. 1. $P(\omega)$ for $\Delta=0.1$ ($J_{\perp}=0.10397$), $\alpha=0.1$ ($J_{\parallel}=4.698$), solid line, and $\alpha=0.2$ ($J_{\parallel}=3.12759$), dashed line. Energies are in units of $D=\omega_c/2=1$. The relation between the AKM parameters $J_{\perp,\parallel}$ and the spin-boson model parameters α,Δ is given in the text. Renormalizations of these parameters due to the discretization of the AKM model have been described in Ref. 24.

where T_K is the low-energy scale of the AKM (or the renormalized tunneling amplitude Δ_r , in the language of the spin-boson model). However, the exponent with which the matrix elements $\langle m'_F | m_{l,GS} \rangle_N$ vanish will also influence the range of validity. We find, by keeping only one energy shell for each frequency ω , that $P(\omega) \sim C_{0r}(\omega)/\omega \sim |\omega|^{\alpha/2}$, $|\omega| \ll \Delta_r$ (noticeable in the low-energy part of our results in Figs. 1 and 2, presented in the next section). The vanishing of $P(\omega)$ with $\omega \rightarrow 0$ reflects the orthogonality of the matrix elements in the expression for $P(\omega)$ and we see that the exponent governing this is $\alpha/2$. The exact behavior of $P(\omega)$ and $C_{0r}(\omega)$ for $\omega \rightarrow 0$ is not rigorously known. In special cases, such as at the Toulouse point, $\alpha=1/2$, it is known that $P(\omega \rightarrow 0) \sim [C_{0r}(\omega)/\omega]_{\omega \rightarrow 0} \sim \text{const}$, and $P(t) \sim e^{-at}$, $t \rightarrow \infty$. This type of exponential relaxation is expected for other α in the range $0 < \alpha < 1$. In any case, we see that the approximate evaluation of the nonequilibrium dynamics taking just one energy shell into account for each frequency is expected to be accurate for weak dissipation (when the overlap exponent is small) and for energies which are not too

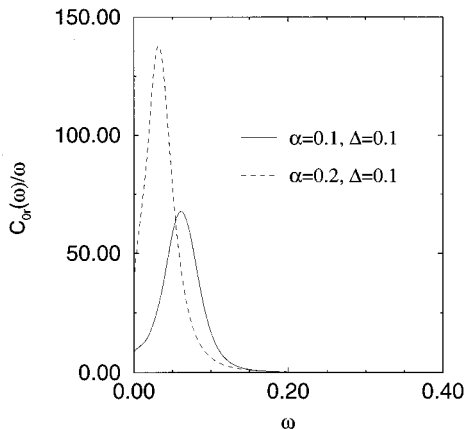


FIG. 2. $C_{0r}(\omega)$ for $\Delta=0.1$ ($J_{\perp}=0.10397$). (a) $\alpha=0.1$ ($J_{\parallel}=4.698$), solid line, and (b) $\alpha=0.2$ ($J_{\parallel}=3.12759$), dashed line. Energies are in units of $D=\omega_c/2=1$.

small relative to Δ_r . In the context of macroscopic quantum coherence experiments in SQUID's, one is interested in the short-time dynamics for times up to approximately $1/\Delta_r$. The long-time behavior $t \gg 1/\Delta_r$ is of interest in other contexts (e.g., microscopic two-level systems), and for these it will be necessary to carry out the full calculation, including higher energy shells, for the nonequilibrium dynamics. We expect that such a calculation will give results as accurate as those for equilibrium quantities.²⁴

IV. RESULTS

For weak dissipation, $\alpha \ll 1$, one expects damped oscillations of the two-level system at a frequency reduced relative to the bare tunneling frequency, Δ , due to the coupling to the environment. From Fig. 1, which shows $P(\omega)$, we see that this expected behavior is reproduced by our method. The presence of an inelastic peak in $P(\omega)$ at $\omega = \Delta_r^*$ indicates damped oscillations of frequency Δ_r^* . The width, γ_r^* of the inelastic peak gives the characteristic time $1/\gamma_r^*$ for the decay of the oscillations. For $\alpha \ll 1$ we find a renormalized tunneling frequency $\Delta_r^* \approx \Delta_r < \Delta$ with $\Delta_r = \Delta [\Delta/\omega_c]^{\alpha/(1-\alpha)}$, and Δ_r is the relevant low-energy scale for weak dissipation as obtained within the NIBA and several other approaches (Refs. 34,35). The larger renormalization of the tunneling amplitude with increasing dissipation is clearly seen in Fig. 1. Qualitatively similar results are found for the quantity $C_{0r}(\omega)/\omega$ (shown in Fig. 2). For weak dissipation, the inelastic peak width $\gamma_r^* \sim \alpha \Delta_r^*$ vanishes linearly with α^{20} . Consequently, for $\alpha \ll 1$, the use of a logarithmic discretization does not provide the necessary resolution at the peak position which is needed for resolving the intrinsic peak width, i.e. any broadening of the discrete spectra will overestimate the inelastic peak width. This problem may be overcome by averaging over discretizations using the procedure in Ref. 33. The standard procedure used here gives correctly the positions and weights of the δ functions in the discrete spectra (this has been shown in detail for all α in the range $0 < \alpha < 1$ for the case of equilibrium dynamical quantities²⁴). The decay of the weights of the δ functions with increasing energy and hence the frequency dependence of $P(\omega)$ at energies $\Delta_r < \omega < \omega_c$ is also correctly captured by our procedure. We find that $P(\omega) \sim C_{0r}(\omega)/\omega \sim \omega^{-(3-2\alpha)}$ for $\Delta \ll \omega_c$, $\Delta_r \ll \omega \ll \omega_c$ and for $0 < \alpha < 1$ (the error in the exponent is typically less than 0.1%). Thus, the short-time behavior of $P(t)$ is identical to the NIBA result $P(t) = 1 - ct^{2(1-\alpha)}$ for $\omega_c^{-1} \ll t \ll \Delta_r^{-1}$. This gives independent confirmation that the NIBA is correct for $P(t)$ at short times.

Hence for weak dissipation we recover the known picture^{19,20} of damped oscillations at reduced tunneling frequency Δ_r . In particular, the short-time dynamics is non-trivial in the sense that $P(t)$ and correlation functions depend on α -dependent exponents. On increasing the dissipation strength, the inelastic peak in $P(\omega)$ narrows and the incoherent contribution [$P(\omega=0)$] becomes larger. For sufficiently strong dissipation, we expect the incoherent part of $P(\omega)$ to dominate and lead to incoherent dynamics of the two-level system. Although the question of the crossover from coherent to incoherent dynamics in equilibrium quantities has

been investigated with high accuracy using the NRG,²⁴ the same question is technically more difficult for nonequilibrium quantities such as $P(\omega)$. In this paper we have calculated the nonequilibrium dynamics only approximately, and the approximation used, which we described in detail in Sec. III C, has a range of validity which restricts us to weak dissipation and energies which are comparable to or higher than the low-energy scale of the model. To address the question of a crossover from coherent to incoherent dynamics we need to evaluate $P(\omega)$ taking into account several energy shells for each frequency ω , as detailed in Sec. III C.

V. CONCLUSIONS

To summarize, we have presented a numerical renormalization-group approach to the calculation of nonequilibrium Green functions in correlated impurity systems. The approach uses an analogy to the calculation of response functions in the x-ray problem where the disturbance is sudden. The method was illustrated by calculating the nonequilibrium dynamics of the Ohmic two-state system. An approximate evaluation of the nonequilibrium quantities, taking only one energy shell into account for each frequency range, gave

accurate results within the expected range of validity of the approximation: specifically, the approximate evaluation of $P(t)$ gave $P(t) = 1 - ct^{2(1-\alpha)}$ for $\omega_c^{-1} \ll t \ll \Delta_r^{-1}$ for all dissipation strengths provided $\Delta \ll \omega_c$. This is in agreement with the NIBA prediction, which is known to be accurate at short times. Including additional energy shells in the evaluation of nonequilibrium quantities should give essentially exact results. This is left for future work as it requires a modified NRG procedure (as discussed in Sec. III C). The method is nonperturbative and can be used to study the effects of local interactions on the nonequilibrium transport through small devices such as quantum dots and tunnel junctions. An important aspect of the method is that the disturbance (an electric or magnetic field) can be arbitrarily large, so it may be used to study the nonlinear regime in the I - V characteristics of small devices, such as quantum dots.

ACKNOWLEDGMENTS

We acknowledge useful discussions with P. Wölfle, Ph. Nozières, and T. Martin. This work was supported by E.U. Grant No. ERBCHRX CT93-0115 and the Institut Laue-Langevin.

*Electronic address: tac@tkm.physik.uni-karlsruhe.de

†Present address.

¹ *Quantum Dynamics of Submicron Structures*, Vol. E291 of Nato ASI Series, edited by H. A. Cerdeira, B. Kramer, and G. Schön (Kluwer, Dordrecht, 1995).

² *Mesoscopic Phenomena in Solids*, edited by B. Altshuler, P. A. Lee, and R. Webb (North-Holland, Amsterdam, 1991).

³ A. K. Geim *et al.*, Phys. Rev. Lett. **72**, 2061 (1994).

⁴ S. M. Girvin, L. I. Glazman, M. Jonson, D. R. Penn, and M. D. Stiles, Phys. Rev. Lett. **64**, 3183 (1990); M. H. Devoret, D. Esteve, H. Grabert, G.-L. Ingold, H. Pothier, and C. Urbina, *ibid.* **64**, 1824 (1990).

⁵ K. A. Matveev and A. I. Larkin, Phys. Rev. B **46**, 15 337 (1992).

⁶ T. K. Ng and P. A. Lee, Phys. Rev. Lett. **61**, 1768 (1988).

⁷ L. I. Glazmann and M. E. Raikh, JETP Lett. **47**, 452 (1988).

⁸ Y. Meir, N. Wingreen and P. A. Lee, Phys. Rev. Lett. **66**, 3048 (1991); Y. Meir, N. Wingreen, and P. A. Lee, *ibid.* **70**, 2601 (1993).

⁹ N. Wingreen and Y. Meir, Phys. Rev. B **49**, 11040 (1994).

¹⁰ S. Hershfield, J. H. Davies, and J. W. Wilkins, Phys. Rev. Lett. **67**, 3720 (1991); Phys. Rev. B **46**, 7046 (1992).

¹¹ J. König, H. Schoeller, and G. Schön Phys. Rev. Lett. **76**, 1715 (1996).

¹² L. V. Keldysh, Sov. Phys. JETP **20**, 1018 (1965).

¹³ L. P. Kadanoff and G. Baym, *Quantum Statistical Mechanics* (Benjamin, New York, 1962).

¹⁴ K. G. Wilson, Rev. Mod. Phys. **47**, 773 (1975).

¹⁵ H. B. Krishnamurthy, J. W. Wilkins, and K. G. Wilson, Phys. Rev. B **21**, 1044 (1980).

¹⁶ P. Nozières and C. T. De Dominicis, Phys. Rev. **178**, 1097 (1969).

¹⁷ A. O. Caldeira and A. J. Leggett, Ann. Phys. (N.Y.) **149**, 374 (1984); **153**, 445(E), (1984).

¹⁸ S. Chakravarty and S. Kivelson, Phys. Rev. Lett. **50**, 1811 (1983); S. Chakravarty and A. J. Leggett, *ibid.* **52**, 5 (1984); A. Garg, Phys. Rev. B **32**, 4746 (1985).

¹⁹ A. J. Leggett, S. Chakravarty, A. T. Dorsey, M. P. A. Fisher, A. Garg, and W. Zwerger, Rev. Mod. Phys. **59**, 1 (1987); **67**, 725 (1995).

²⁰ U. Weiss, *Series in Modern Condensed Matter Physics* (World Scientific, Singapore, 1993), Vol. 2.

²¹ G. Toulouse, C.R. Acad. Sci. **268**, 1200 (1969).

²² P. B. Viggmann and A. M. Finkel'stein, Sov. Phys. JETP **48**, 102 (1978); P. Schlottmann, Phys. Rev. B **25**, 4805 (1982).

²³ F. Guinea, V. Hakim, and A. Muramatsu, Phys. Rev. B **32**, 4410 (1985).

²⁴ T. A. Costi and C. Kieffer, Phys. Rev. Lett. **76**, 1683 (1996).

²⁵ G. Kotliar and Q. Si, Phys. Rev. B **53**, 12 373 (1996).

²⁶ P. W. Anderson, G. Yuval, and D. R. Hamann, Phys. Rev. B **1**, 4464 (1970).

²⁷ A. M. Tselvelick and P. B. Wiegmann, Adv. Phys. **32**, 453 (1983).

²⁸ F. Lesage, H. Saleur, and S. Skorik, Phys. Rev. Lett. **76**, 3388 (1996).

²⁹ T. A. Costi, A. C. Hewson, and V. Zlatić, J. Phys. Condens. Matter **6**, 2519 (1994); T. A. Costi, and A. C. Hewson, *ibid.* **5**, 361 (1993); Philos. Mag. B **65**, 1165 (1992).

³⁰ This symmetry is a consequence of the local exchange interactions and the particle-hole symmetry of the conduction band. It was used in NRG calculations in the context of the two-impurity Kondo problem, B. Jones, C. M. Varma, and J. W. Wilkins, Phys. Rev. Lett. **61**, 125 (1988).

³¹ This is due, first, to the absence of the above symmetries which would substantially increase the size of the matrices that need to be diagonalized, and, second, in the corresponding linear chain model for a bosonic heat bath each orbital b_n (corresponding to $f_{n\mu}$ in the fermionic case) can be occupied with arbitrary number of bosons. This would require an additional approximation to be made, restricting the number of such bosons in each orbital b_n to a finite number.

³² P. W. Anderson, Phys. Rev. Lett. **18**, 1049 (1967).

- ³³M. Yoshida, M. A. Whitaker, and L. N. Oliveira, Phys. Rev. B **41**, 9403 (1990); W. C. Oliveira and L. N. Oliveira, *ibid.* **49**, 11986 (1994).
- ³⁴This energy scale also appears as a scaling invariant of the Anderson-Yuval scaling equations for the AKM in the limit $J_{\parallel} \rightarrow \infty$, which corresponds to $\alpha \rightarrow 0$ in the spin-boson model (Refs. 19 and 26).
- ³⁵S. K. Kehrein, A. Mielke, and P. Neu, Z. Phys. B **99**, 269 (1996); S. K. Kehrein and A. Mielke, Ann. Phys. (Leipzig) (to be published).